

## **SECTION 1**

### **INTRODUCTION**

Nonstructural components anchored or attached to a building structure are generally considered as those elements that are not a part of the load-bearing structural system. They include mechanical and electrical equipment, architectural elements, and building contents. The importance of nonstructural component issues in seismic design and performance evaluation is now well recognized by researchers as well as practicing engineers. The subject received special attention after the San Fernando earthquake of 1971 when it became clear that nonstructural damage not only can result in major economic loss, but also can pose real threat to life safety.

Today, major building codes and seismic design guidelines exist which address seismic design forces for various nonstructural components. The 1991 NEHRP provisions [7] and 1991 UBC code [13], for example, are widely used for seismic design standards for nonstructural components, from which local jurisdictions and some federal agencies have developed similar seismic design requirements. In these provisions, the design force for nonstructural components is formulated as an equivalent static lateral force applied to the approximate center of gravity of the component being analyzed. While simple formulas are necessary for the sake of design applications, they contain considerable amount of arbitrariness and subjectivity which produce ambiguous results and inconsistent design forces among different codes and provisions. Furthermore, they do not reflect the level of understanding of the behavior of nonstructural components that has been achieved through theoretical analyses, experiments, and observation data from past earthquakes.

The thrust of this work is to critically assess current design force formulas for nonstructural components as they exist in the 1991 NEHRP provisions, to identify their shortcomings, and to recommend revisions which would bring them more in line with current state-of-the-knowledge in this area. These revisions are recommended within the framework of the equivalent lateral force format for practical applicability.

The 1991 NEHRP design force formulas for nonstructural components are reviewed in Section 2 and their shortcomings are identified and commented upon. Three revision recommendations based on incorporation of different levels of consideration of structural and component effects are advanced in Sections 3-5. It is shown that these revisions can

be justified on the basis of simple dynamic analyses, experimental results, and experience data.

In Section 6, these three recommended design force formulas are compared among themselves as well as in relation to existing codes and provisions. These results are further examined through case studies.

Since excessive displacements on the part of nonstructural components are causes of failure in a large number of cases during past earthquakes, the derivation of simple displacement equations for support deformation and sliding is considered in Section 7. It is recommended that this type of displacement equations be added to future codes and provisions in order to achieve a more complete seismic design scenario for nonstructural components.

## SECTION 2

### AN ASSESSMENT OF 1991 NEHRP PROVISIONS

#### 2.1 Brief Summary of Current Design Forces

In 1991 NEHRP Provisions [7], as in other codes such as the 1991 UBC [13] or the 1985 Tri-Service Manual [25], seismic design forces for nonstructural components are specified in terms of static equivalent forces acting through their centers of gravity. They are described below for architectural components and for mechanical and electrical components.

##### 2.1.1 Architectural Components

Architectural components and their means of attachment are designed for seismic forces ( $F_p$ ) determined in accordance with the following equation:

$$F_p = A_v C_c P W_c \quad (2.1)$$

in which:

$F_p$  is the seismic force applied to a component of a building at its center of gravity;

$A_v$  is the seismic coefficient representing effective peak-velocity related acceleration from Sec. 1.4.1 of [7];

$C_c$  is the seismic coefficient for architectural components from Table 8.2.2 of [7];

$P$  is the performance criteria factor from Table 8.2.2 of [7]; and

$W_c$  is the weight of the architectural component.

The force ( $F_p$ ) is applied independently at vertical, longitudinal, and lateral directions in combination with the static load of the element.

##### 2.1.2 Mechanical and Electrical Components

Mechanical and electrical components and systems are designed for seismic forces determined in accordance with the following equation:

$$F_p = A_v C_c P a_c W_c \quad (2.2)$$

in which:

$F_p$  is the seismic force applied to a mechanical or electrical component at its center of gravity;

$C_e$  is the seismic coefficient for mechanical and electrical components from Table 8.3.2a of [7];

$P$  is the performance criteria factor from Table 8.3.2a of [7];

$a_c$  is the amplification factor determined in accordance with Table 8.3.2b of [7]; and

$w_e$  is the operating weight of the mechanical or electrical component or system.

Alternatively, the seismic forces ( $F_p$ ) can be determined by a properly substantiated dynamic analysis subject to approval by the building code official.

### **2.1.3 Comments on the Seismic Coefficient ( $C_e$ )**

The specification of the component seismic coefficient ( $C_e$ ) in Eq. (2.1) was originally based on the use of the working stress design and was similar to the  $C_p$  factors specified in the UBC (1991) [13] and Title 24 of the California Administrative Code [24]. The values of  $C_p$  in the UBC (1991) [13] were set basically by professional judgement, primarily from examining the performance of equipment in past earthquakes. Some results from analyses of linear elastic multistory buildings were used to justify general relationships among the various values. Additional capacity and ductility reservations were permitted in the assignment of the  $C_p$  values [20]. Based on these observations, the determination of the  $C_e$  values is basically a subjective result from experts in the related fields and their assigned values are somewhat arbitrary.

For the design of the mechanical and electrical equipment, the seismic coefficient ( $C_e$ ) in Eq. (2.2) was originally introduced to represent an amplification of the effective peak acceleration coefficient for coefficient  $A_v$  equal to or greater than 0.2 ([7], Part 2, p. 183). In order to bring  $C_e$  into conformance with other sections of the provisions. The concept was changed by defining  $C_e$  as a numerical dimensionless factor related to that for mechanical and electrical components in Table 8.3.2a of [7]. The values presented in the table were developed by adopting an analogy to the  $C_p$  values in Table T17-23-3 of Title 24 of the California Administrative Code [24] with the consistent performance criteria level of the 1991 NEHRP Provisions taken into account.

To sum up, the component seismic coefficient ( $C_e$ ) in Eqs. (2.1) and (2.2) appears to be a subjectively-assigned, reflecting in part the component performance during past

strong earthquakes. The determination of this value may involve many factors, including the attachment and constraint detailing effect, transient characteristics of the seismic input, uncertainties in the determination of amplification factor ( $a_e$ ), interaction between the component and its supporting structure, soil property and structural behaviors, etc. Based on different interpretations of these effects on the determination of  $C_e$ , three approaches are proposed in this report to revise formulation of the seismic design force for nonstructural components.

## **2.2 Shortcomings of Current Provisions**

A design provision provides minimum legal design requirements for building structures. Without sacrificing simplicity for applicability to practical design, the design guidelines should reflect the state-of-the-knowledge as well as accumulated experience. As mentioned in the Introduction, the 1991 NEHRP Provisions in the area of nonstructural components have not kept in pace with current understanding of their seismic behavior through analyses, experiments, and field observations. This implies inadequacies of the current provisions in providing basic design requirements such as the minimum design forces. The major deficiency in the design force formulas for nonstructural components appears to be the negligence of their supporting structural behaviors. In particular, effects of soil type, structural period, component location and structural yielding on the nonstructural element design are not included. The anchorage detailing of the nonstructural component might be implied in the seismic coefficient ( $C_e$ ) but has not been interpreted on physical grounds.

### **2.2.1 Soil Type Effect**

In the current provisions, the design force on the nonstructural element attached to a building structure is considered to be independent of the soil type, as can be seen in Eqs. (2.1) and (2.2). Obviously, this is inconsistent with design requirements for building structures. As evidenced in the design of a building structure [7,13], soil condition has a great influence on the design base shear force for the building structure. The softer the soil layer on which the building structure is constructed, the more stringent the design requirement for the building structure. Since the seismic input to a nonstructural element is the dynamic response at its supporting locations in the building structure, its seismic response clearly depends on the properties of soils supporting the building structure. Furthermore, effects of site conditions on the design for building structures have also been amply demonstrated by past earthquake observations [26].

### **2.2.2 Location Effect**

According to current provisions, nonstructural components located at different floors of a supporting structure are designed for the same level of force. In practice, however, nonstructural elements attached to different floors of the supporting building structure will experience different levels of acceleration. The floor amplification effect can be observed from past earthquakes as well as from analytical results as shown in Section 3.2. The inclusion of the floor amplification effect in the design force formulas of the two earlier editions of NEHRP (1985 [5] and 1988 [6]) also demonstrates the need for distinguishing design forces on nonstructural elements situated on different floors, though the effect was discarded in the 1991 edition in favor of a somewhat arbitrarily defined  $C_e$  coefficient.

### **2.2.3 Structural Period Effect**

For the design of architectural components, the design force ( $F_p$ ) in Eq. (2.1) is not considered to be related to the structural period ( $T_s$ ). However, design forces on the architectural components obviously require the distinction between flexible and stiff building structures as can be seen in the base shear force formula for building structural design. For instance, a flexible structure may receive a small amount of inertia force so that an architectural component or mechanical equipment rigidly mounted to the structure are only slightly excited. As discussed in Section 3.2.3, the distribution of the acceleration or inertia force along the building height is also different for building structures with different periods.

The same is also true of the structural period effect on the design force for mechanical and electrical equipment, Eq. (2.2). Although the structural period ( $T_s$ ) is incorporated into the amplification factor ( $a_c$ ) in Eq. (2.2), it accounts for only partial effect that structural period has on the equipment response.

### **2.2.4 Structural Yielding Effect**

Effects of structural yielding on the structural and nonstructural component design are considerably different. A building structure may experience inelastic deformation during severe earthquakes and, indeed, yielding of the building structure is considered as a limit state for its own design in the current provisions. However, this may not be the case for the design of nonstructural components. Failure of a nonstructural component attached to a building structure situated in a high seismic zone can occur under either of the following two cases: (1) the structure behaves inelastically under the maximum earthquake input at

the site; or (2) the structure remains elastic during a small or moderate earthquake input at the same site. Yielding of the building structure will absorb a substantial amount of energy and hence reduce the seismic force imposed on the structure, however, the seismic input energy into the nonstructural component depends both on the direct seismic energy through seismic inertia force and the transferred energy from the supporting building structure. Under a strong earthquake, the direct seismic energy from the earthquake may be large but the transferred energy from the supporting structure is usually small due to structural yielding. On the other hand, the direct seismic energy under a small or moderate earthquake is relatively small and the transferred energy can be relatively large so that the total energy received by the nonstructural component might be greater than that under a strong earthquake.

#### **2.2.5 Anchorage Detailing Effect**

Finally, anchorage detailing of nonstructural components can also have a significant influence on the design forces. As has been observed, damage of a nonstructural component in many cases results from the failure of its anchorage due to excessive stress. An appropriate design for anchorage detail can thus significantly improve the nonstructural component's performance during earthquakes. For example, the introduction of ductility capacity in the anchorage will reduce the design force.

These observations have led to three recommendations for the revision of 1991 NEHRP Provisions for architectural, mechanical, and electrical components as described in the following sections.

## SECTION 3

### FIRST RECOMMENDATION

In this approach, the value of  $C_e$  is considered to be affected by the interaction between the component and its supporting structure, soil properties, structural behavior, uncertainties in determination of the amplification factor, and transient characteristics of seismic input as well as the equipment detailing effect or yielding potential of mechanical or electrical equipment.

It is noted that the first four factors discussed in the shortcomings of nonstructural component design formulas outlined in Section 2.2 have been incorporated into the base shear of structural design in the current provisions. It is thus natural to take into account these effects in mechanical or electrical equipment design by transferring the vertical distribution of the base shear along the building structural height to the equipment.

### 3.1 Suggested Revision of the Design Force

#### 3.1.1 Design Force Equation

Mechanical and Electrical Equipment. It is proposed that mechanical and electrical components and system be designed for seismic force determined in accordance with the following equation:

$$F_p = C_p W_c \quad (3.1)$$

in which  $F_p$  and  $W_c$  are, respectively, the seismic force applied to a nonstructural component at its center of gravity and the weight of the component as defined in the current provisions, and  $C_p$  is the seismic design coefficient of the nonstructural component which can be calculated from

$$C_p = \frac{A_v a_x a_c P}{R_s R_c} \quad (3.2)$$

where  $a_x$  is the floor amplification factor which can be determined by (see Fig. 3-1)

$$a_x = 1 + \frac{h_x}{h_n} (a_n - 1) \quad (3.3)$$

with

$$a_n = 1.5 \beta_s \geq 1 \quad (3.4)$$



and

$$\beta_s = \frac{1.2S}{T_s^{2/3}} \leq \frac{2.5A_a}{A_v} \quad (3.5)$$

in which  $S$  is the site coefficient from Table 3-2 in [7],  $A_v$  and  $A_a$  are, respectively, the effective peak velocity-related acceleration and the effective peak acceleration from Section 1.4.1 of [7], and  $T_s$  is the structural period determined in Section 4.2.2 of [7].

The factor  $a_c$  in Eq. (3.2), a function of period ratio ( $T_c/T_s$ ) between equipment and its supporting structure, is the equipment amplification factor which can be calculated by (see Fig. 3-2)

$$a_c = \begin{cases} 1.0, & T_c/T_s \leq 0.5 \text{ and } T_c/T_s \geq 2.0 \\ 2.5, & 0.7 \leq T_c/T_s \leq 1.4 \\ -2.75 + 7.5(T_c/T_s), & 0.5 < T_c/T_s < 0.7 \\ 6 - 2.5(T_c/T_s), & 1.4 < T_c/T_s < 2.0 \end{cases} \quad (3.6)$$

The factor  $R_s$  in Eq. (3.2) is the response modification coefficient for component design due to structural yielding which can be estimated from the response modification coefficient for structural design ( $R$ ) in Table 3-3 of [7] by

$$R_s = 1 + \frac{R - 1}{7} \quad (3.7)$$

Its values are tabulated in Table 3-1 in this report for different types of buildings. In Eq. (3.2), the performance criteria factor ( $P$ ) takes different values than those in the current provisions as shown in Table 3-2 and  $R_c$  is the response modification coefficient due to component yielding which is tentatively presented in Table 3-2.

**Architectural Components.** For architectural components, the design force ( $F_p$ ) is again expressed by Eq. (3.1) except that the equipment amplification factor ( $a_c$ ) is assigned to be 1.0 and the performance criteria factor ( $P$ ) and the response modification coefficient ( $R_c$ ) take different values as presented in Table 3-3.

### 3.1.2 Development of the Design Force Equation

In this section, the formulation of  $C_p$  in Eq. (3.2) is discussed in detail. Since  $C_p$  is closely related to the base shear and force distribution of the supporting structure, formulas for their calculations are also given.

**Base Shear Force for Structure.** The seismic base shear force ( $V$ ) of the building structure in a given direction is provided by Eq. (4-1) in [7], i.e.,

$$V = C_s(W_s + W_c) \quad (3.8)$$

in which  $w_s$  is the total dead load and applicable portion of other loads on the building structure and the seismic design coefficient  $C_s$  can be written as (Eq. (4-2) of [7])

$$C_s = \beta_s \cdot \frac{A_v}{R_s} \quad (3.9)$$

Here,  $R_s$  is the modified response modification coefficient ( $R$ ) for building structures defined in Table 3-3 of [7]. This modification is necessary because the reserve capacity for building structure design due to nonstructural element constraint and unnecessary redundancy no longer exists for nonstructural element design and the ductility capacity for structural design is not totally transferable to the nonstructural component design. A very simple modification would be to shrink the response modification coefficient ( $R$ 's) for structural design into the range from 1.0 to 2.0 for nonstructural component design as given in Eq. (3.7). The quantity  $\beta_s$  is a coefficient which is actually related to the seismic response spectrum as given by Eq. (3.5), which is derived from Eq. (4-2) of [7].

Vertical Distribution of Base Shear Force. As shown in Fig. 3-3, the total base shear force ( $V$ ) is balanced by the seismic force on mechanical and electrical equipment ( $F_p$ ) and the inertia force on building floors ( $F_i$ ,  $i = 1, 2, \dots, n$ ), i.e.,

$$V = F_p + \sum_{i=1}^n F_i \quad (3.10)$$

Assuming that the inertia force acting on a given floor is proportional to the floor height multiplied by its floor weight as in the structural design in the current provisions, the inertia force acting on the floor at  $h_x$  level can be then formulated as

$$F_x = C_{vx}(V - F_p) \quad (3.11)$$

in which the vertical distribution factor ( $C_{vx}$ ) can be expressed as

$$C_{vx} = \frac{W_x(h_x + h_0)}{\sum_{i=1}^n W_i(h_i + h_0)} = \frac{W_x a_x}{\sum_{i=1}^n W_i a_i} \quad (3.12)$$

and

$$h_0 = \frac{h_n}{a_n - 1} \quad (3.13)$$

as denoted in Fig. 3-1. The quantity  $h_0$  is introduced because the acceleration distribution along building height is trapezoidal instead of triangular as will be illustrated in Section 3.2.

Design Force on Equipment at  $h_x$  Level. The floor acceleration can be calculated by dividing the lateral force ( $F_x$ ) by its floor mass. This acceleration is amplified by  $a_c$  to obtain the equipment acceleration which is then multiplied by equipment mass to arrive at the design force on the equipment attached to the floor at  $h_x$  level, i.e.,

$$F_p = \left( \frac{F_x}{W_x} \right) a_c W_c \quad (3.14)$$

or

$$F_x = \frac{W_x F_p}{W_c a_c} \quad (3.15)$$

As one can see from Eqs. (3.11) and (3.12), the ratio of the inertia forces between the  $i$ th floor and the  $x$ th floor is

$$\frac{F_i}{F_x} = \frac{W_i a_i}{W_x a_x} \quad (3.16)$$

By substituting Eq. (3.15) for  $F_x$  in Eq. (3.16), the inertia force on the  $i$ th floor ( $F_i$ ) can be expressed as

$$F_i = \frac{W_i a_i}{W_x a_x} F_x = \frac{W_i a_i}{W_c a_c a_x} F_p \quad (3.17)$$

Consequently, the seismic force on the equipment ( $F_p$ ) can be determined by introducing Eq. (3.17) into Eq. (3.10), giving

$$F_p = \frac{V}{1 + \frac{1}{a_c a_x} \sum_{i=1}^n \frac{W_i}{W_c} a_i} = \frac{A_v a_c a_x W_c}{R_s} \alpha_1 \alpha_2 \quad (3.18)$$

in which

$$\alpha_1 = \frac{\beta_s}{\sum_{i=1}^n \frac{W_i}{W_s} a_i} \quad (3.19)$$

$$\alpha_2 = \frac{\left(1 + \frac{W_c}{W_s}\right) \sum_{i=1}^n \frac{W_i}{W_s} a_i}{\frac{W_c}{W_s} a_c a_x + \sum_{i=1}^n \frac{W_i}{W_s} a_i} \quad (3.20)$$

where Eqs. (3.8) and (3.9) have been employed.

For a uniform building structure, i.e.,  $W_s = nW_1$  and  $h_n = nh_1$ , coefficients  $\alpha_1$  and  $\alpha_2$  can be respectively written as

$$\alpha_1 = \frac{2\beta_s}{a_n + 1 + (a_n - 1)/n} \quad (3.21)$$

$$\alpha_2 = \frac{\left(1 + \frac{W_c}{W_s}\right) \left(\frac{a_n+1}{2} + \frac{a_n-1}{2n}\right)}{\frac{W_c}{W_s} a_c a_x + \frac{a_n+1}{2} + \frac{a_n-1}{2n}} \quad (3.22)$$

When a moment-resistent frame structure with the estimated fundamental period ( $T_s$ ) equal to 0.1n sec (Eq. (4-4a) of [7]) is constructed on soil layer of type 1, coefficient  $\alpha_1$  is plotted in Fig. 3-4 against structural period  $T_s$ . As one can see,  $\alpha_1$  almost remains constant and is approximately equal to 0.9. Therefore, coefficient  $\alpha_1$  can be approximately set to 1.0 for simple design purposes for this type of uniform structures.

Equation (3.22) shows that coefficient  $\alpha_2$  is a function of mass ratio  $W_c/W_s$ , period ratio  $T_c/T_s$  implied in  $a_c$ , and position  $x$  expressed by  $a_x$ , which can be defined as an interaction factor. When  $a_x \cong [a_n + 1 + (a_n - 1)/n]/2$ , interaction factor  $\alpha_2$  is plotted in Fig. 3-5 as a function of mass ratio  $W_c/W_s$  for both detuned and tuned cases, indicating that seismic force acting on an equipment ( $W_c = 0.1W_s$ ) can be reduced by about 12% due to the interaction effect in the tuned case. Following simplicity requirements for practical design, the interaction effect can be neglected for light equipment and therefore the seismic force on the equipment is simply represented by

$$F_p = \frac{A_v a_x a_c W_c}{R_s} \quad (3.23)$$

Ductility Capacity of Equipment. As in structural design, the seismic force in Eq. (3.23) can be reduced by a factor  $R_c$  for equipment design due to potential ductility capacity in the equipment anchorage, hence,

$$F_p = \frac{A_v a_x a_c W_c}{R_s R_c} \quad (3.24)$$

Performance Criteria Factor. By considering the performance criteria factor ( $P$ ) for equipment, the design force on the equipment can be finally formulated as

$$F_p = \frac{A_v a_x a_c P W_c}{R_s R_c} = C_p W_c \quad (3.25)$$

### 3.1.3 Performance Criteria Factor (P) and Response Modification Coefficient ( $R_c$ )

As illustrated by the derivations given above, characteristics of an integrated system consisting of nonstructural elements and building structure show that the nonstructural element performance during earthquakes can be considerably improved. Impact of the nonstructural element importance (or function) on the design of the nonstructural element should therefore be not as significant as that in the current provisions. The values of 0.8, 1.0, 1.2 for the performance criteria factor ( $P$ ) are thus suggested for architectural components as well as mechanical and electrical components with seismic

hazard exposure group I, II, and III, respectively. The specific values of  $P$  for different nonstructural elements can be obtained by modification of the number in Tables 8-2-2 and 8-3-2(a) of [7] and are retabulated in Tables 3-2 and 3-3 here.

The response modification coefficients ( $R_c$ 's) can be determined by following two steps: (1) direct transfer of the seismic coefficients ( $C_c$ ) in the current provisions to  $\bar{R}_c$  and (2) modification of the obtained values ( $\bar{R}_c$ ) to obtain  $R_c$ . Here,  $\bar{R}_c$  accounts for effects of both structure and component on the design force of the nonstructural component; whereas  $R_c$  takes into account the nonstructural component effects only. The relationship between  $R_c$  and  $\bar{R}_c$  can be simply established as

$$R_c = 1 + \frac{2}{3}(\bar{R}_c - 1) \quad (3.26)$$

which compresses the range (1 - 4.5) of  $\bar{R}_c$  into the range (1 - 3) of  $R_c$ . The determination of  $\bar{R}_c$  is discussed in Section 5.1.3.

#### 3.1.4 Comments on Structural Yielding Effect

As pointed out in Section 2.2.4, structural yielding does not necessarily cause the maximum seismic force acting on a nonstructural component attached to the structure. This phenomenon is not reflected in the design force formula (Eq. (3.1)) for simplicity. If warranted, this effect can be included in the design force computation by adding the constraint

$$\frac{A_v}{R_s} \geq \min(A_v, A_{vy}) \quad (3.27)$$

in which  $A_{vy}$  denotes the peak velocity-related acceleration resulting in structural yielding. In an earthquake-prone area,  $A_v$  could be larger than  $A_{vy}$  and Eq. (3.27) basically means that the larger of the input accelerations of a structure in the inelastic state and in the initial yielding state should be used as the input for nonstructural component design.

### 3.2 Justifications

In formulating the recommended revision to the current provisions, efforts have been made to incorporate into the revision the latest theoretical research results and available experimental results as well as building response observation data and reconnaissance reports of recent earthquakes.

### 3.2.1 Theoretical Analyses

Modal Shapes and Mass Distribution Factor. For a uniform moment-resisting frame structure as shown in Fig. 3-1, the equation of motion is given by

$$\mathbf{M}\ddot{\mathbf{y}}(t) + \mathbf{C}\dot{\mathbf{y}}(t) + \mathbf{K}\mathbf{y}(t) = -\mathbf{M}\mathbf{e}\ddot{x}_g(t) \quad (3.28)$$

in which  $\mathbf{M}$ ,  $\mathbf{C}$ , and  $\mathbf{K}$  are the mass, damping, and stiffness matrices of an  $n$ -story structure;  $\mathbf{e}$  is the index vector of earthquake input; and  $\mathbf{y}(t)$  is the relative displacement of the structure with respect to the ground. The fundamental period of the structure can be analytically calculated by [8]

$$T_s = \frac{T_0}{2 \sin \left( \frac{\pi}{2(2n+1)} \right)} \quad (3.29)$$

in which  $T_0$  is the period of its associated one-story building. The mode shape associated with the first mode can be analytically formulated as

$$\phi(n) = 1 \quad (3.30)$$

$$\phi(n-1) = 1 - \lambda_1 \quad (3.31)$$

$$\phi(i) = (2 - \lambda_1)\phi(i+1) - \phi(i+2), \quad i = 1, 2, \dots, n-2 \quad (3.32)$$

where

$$\lambda_1 = \left( \frac{T_0}{T_s} \right)^2 \quad (3.33)$$

The first mode shape is shown in Fig. 3-6 for buildings with different numbers of stories ( $n$ ). It can be observed that the mode shape of a frame system is quite stable as the number of story increases and can be approximated by a straight line.

When the first mode shape is assumed to be a straight line, the  $i$ th element of mode shape vector  $\phi$  can be simply expressed as

$$\phi(i) = \frac{i}{n} \quad (3.34)$$

and the modal mass and participation factor can be formulated as

$$m_1 = \phi^T \mathbf{M} \phi = m \sum_{i=1}^n \left( \frac{i}{n} \right)^2 = \frac{m(n+1)(2n+1)}{6n} \quad (3.35)$$

$$\phi \mathbf{M} \mathbf{e} = m \sum_{i=1}^n \frac{i}{n} = \frac{m(n+1)}{2} \quad (3.36)$$

$$\Gamma_1 = \frac{\phi^T \mathbf{M} \mathbf{e}}{\phi^T \mathbf{M} \phi} = \frac{3n}{2n+1} \quad (3.37)$$

The mass distribution factor  $\phi(n)\Gamma_1$  can then be formulated as

$$\phi(n)\Gamma_1 = \frac{3n}{2n+1} \quad (3.38)$$

which approaches 1.5 for large  $n$ , i.e., the factor used in Eq. (3.4).

Absolute Acceleration or Inertia Force Distribution over Building Height. The equation of motion of the first-mode representation of a multi-degree-of-freedom (MDOF) building structure can be expressed by

$$\ddot{y}_x(t) + 2\xi_1\omega_1\dot{y}_x(t) + \omega_1^2 y_x(t) = -\phi(x)\Gamma_1 \ddot{x}_g(t) \quad (3.39)$$

in which  $y_x(t)$  is the relative displacement of the structure at  $h_x$  level and can be further expressed by

$$y_x(t) = \phi(x)\Gamma_1 q(t) \quad (3.40)$$

$$\ddot{q}(t) + 2\xi_1\omega_1\dot{q}(t) + \omega_1^2 q(t) = -\ddot{x}_g(t) \quad (3.41)$$

The absolute acceleration of the structure at  $h_x$  level can thus be formulated as

$$\ddot{y}_x(t) + \ddot{x}_g(t) = \phi(x)\Gamma_1[\ddot{q}(t) + \ddot{x}_g(t)] + [1 - \phi(x)\Gamma_1]\ddot{x}_g(t) \quad (3.42)$$

from which one can readily observe that vertical distribution of the absolute acceleration is trapezoidal if the first mode shape  $\phi(x)$  is assumed to be a straight line. At the base of the building structure,  $\phi(x) = 0$  and  $\ddot{y}_x(t) + \ddot{x}_g(t) = \ddot{x}_g(t)$ , which is exact. The floor amplification factor ( $a_0$ ) in this case is equal to unity. At the top of the structure, the first term in Eq. (3.42) is predominant and therefore the floor amplification factor  $a_n$  is approximately equal to the acceleration response spectrum calculated by Eq. (3.41) multiplied by a mass distribution factor  $\phi(n)\Gamma_1$ . This is the theoretical foundation of Eq. (3.4).

Amplification Factor ( $a_c$ ) and Mass Ratio Effect. The equation of motion for a coupled system with a single-degree-of-freedom (SDOF) representation of the equipment and a SDOF representation of the MDOF structural system can be written as

$$m_x[\ddot{y}_x(t) + 2\xi_1\omega_1\dot{y}_x(t) + \omega_1^2 y_x(t)] - m_c[2\xi_c\omega_c\dot{z}(t) + \omega_c^2 z(t)] = -\phi(x)\Gamma_1 m_x \ddot{x}_g(t) \quad (3.43)$$

$$m_c[\ddot{z}(t) + 2\xi_c\omega_c\dot{z}(t) + \omega_c^2z(t)] = -m_c[\ddot{y}_x(t) + \ddot{x}_g(t)] \quad (3.44)$$

in which the modal mass of the structure represented by the relative displacement at  $h_x$  level is calculated by

$$m_x = \frac{\phi^T \mathbf{M} \phi}{\phi^2(x)} \quad (3.45)$$

$m_c$ ,  $\xi_c$ , and  $\omega_c$  are the equipment mass, damping ratio, and frequency, respectively, and  $z(t)$  is the relative displacement of the equipment with respect to the building floor at  $h_x$  level.

The root-mean-square ratio between absolute accelerations of the equipment and the first mode representation of a six-story uniform moment-resisting frame structure subjected to seismic excitation with the Kanai-Tajimi spectrum (an indication of amplification factor for equipment subjected to random loadings) is plotted in Fig. 3-7 as a function of the period ratio ( $T_c/T_s$ ) and for different mass ratios ( $m_c/m_x$ ) and different  $\phi(x)\Gamma_1$ 's due to different equipment locations. The Kanai-Tajimi spectrum has the form

$$S_{\ddot{x}_g}(\omega) = S_0 \frac{1 + 4\xi_g^2 \left(\frac{\omega}{\omega_g}\right)^2}{\left(1 - \frac{\omega^2}{\omega_g^2}\right)^2 + 4\xi_g^2 \left(\frac{\omega}{\omega_g}\right)^2} \quad (3.46)$$

with parameters  $S_0 = 1$ ,  $\xi_g = 0.64$ ,  $\omega_g = 15.6$  rad/sec [12].

Further examination of Eqs. (3.43) and (3.45) shows that both the mass ratio ( $m_c/m_x$ ) and the mass distribution factor ( $\phi(x)\Gamma_1$ ) increase when floor number on which the equipment is installed increases. The increase of the mass ratio means a reduction of the equipment amplification factor ( $a_c$ ) due to interaction effect while the increase of the mass distribution factor results in greater equipment amplification factor. The question as to whether the floor amplification factor ( $a_x$ ) and the equipment amplification factor ( $a_c$ ) in the design force formula can be separately considered is therefore posed here. A very preliminary conclusion can be drawn from Fig. 3-7, which shows that the equipment amplification factor ( $a_c$ ) can be approximately determined independent of location of the equipment. This supports the derivation process for the design force in the suggested approach.

Uncertainty Effect on the Determination of Amplification Factor ( $a_c$ ). In the above, the equipment amplification factor ( $a_c$ ) of a six-story building structure has been evaluated individually. For design purposes, however, a simpler but more general formulation for  $a_c$



is needed. The simplest model for  $a_c$  would include the determination of both amplitude and broadened band associated with the equipment response spectrum in the tuned case.

The response of mechanical or electrical equipment located on ground or on a very rigid structure is mainly a function of the frequency content of the postulated earthquake, whereas the response of the equipment attached to a relatively flexible structure is mainly a function of the structure's natural periods. The supporting structure in this case acts as a filter amplifying the seismic motion at its own natural periods. The statistical characteristics of the equipment response during a seismic disturbance in the first case can be well described by the design response spectrum value ( $\beta_s$ ), while the equipment response on a flexible structure can be simply described as the harmonic response oscillating at the fundamental structural period. The reality for the determination of  $a_c$  is between the above two extreme cases. Based on these observations, we consider the amplitude of  $a_c$  for all period ratios between the equipment and the structure to be not less than 2.5.

Due to uncertainties involved in the structural parameters such as mass, stiffness, and damping ratio, the peak value of  $a_c$  (commonly called floor response spectrum) needs to be broadened for design purposes. According to the analyses performed for nuclear power plant design [1], coefficients of variation (Cov) of 5-10% for mass determination and about 34% for stiffness determination are appropriate. In what follows, coefficients of variation of the structural period and the equipment period are simply evaluated by assuming perfect correlation between masses at different floors or between stiffnesses at different floors. In this case, the fundamental period of the structure can be calculated by Eq. (3.29) but  $T_0$  in the formula is a random variable.

When mass and stiffness of a uniform structure are considered as two independent lognormal random variables, the coefficient of variation for its fundamental period,  $\text{Cov}(T_s)$ , can be calculated from the coefficient of variation of mass,  $\text{Cov}(M)$ , and of stiffness,  $\text{Cov}(K)$ , by the following equation:

$$\text{Cov}(T_s) = \sqrt{[1 + (\text{Cov}(M))^2]^{1/4} [1 + (\text{Cov}(K))^2]^{1/4} - 1} \quad (3.47)$$

Substituting  $\text{Cov}(M) = 0.10$  and  $\text{Cov}(K) = 0.34$  into Eq. (3.47), we can calculate the coefficient of variation for the structural period, i.e.,  $\text{Cov}(T_s) = 0.174$ . The structural period ( $T_s$ ) in this case is also lognormal. Assuming that the equipment period ( $T_e$ ) has the same coefficient of variation as the structural period but is independent of  $T_s$ , the coefficient of

variation of the period ratio between the equipment and the structure can be subsequently calculated as

$$\text{Cov}(T_c/T_s) = \sqrt{[1 + (\text{Cov}(T_c))^2][1 + (\text{Cov}(T_s))^2] - 1} \quad (3.48)$$

$$= \sqrt{(1 + 0.174^2)^2 - 1} = 0.248 \quad (3.49)$$

Considering nonuniformity of mass and stiffness distributions along the building height, imperfectly-correlated properties associated with masses or stiffnesses at different floors, possible higher-mode effects, and other uncertainty factors such as damping coefficients as well as the fact that both  $\text{Cov}(K)$  and  $\text{Cov}(M)$  might be larger for regular building structures, a coefficient of variation of 30% for the period ratio ( $T_c/T_s$ ) is suggested. That is, the peak value of  $a_c$  can be broadened into the range of 0.7 to 1.3. However, sensitivity of the period ratio to uncertainties existed in the equipment-structure system is often stronger for flexible equipment than for stiff equipment and the amplification factor always skews toward the larger period ratio ( $T_c/T_s$ ) as illustrated in Fig. 3-7. The peak value is finally recommended to be broadened to the range of 0.7 to 1.4. From recent research on decoupling criteria between equipment and structure [8] and other related research results, the interaction effect outside the range of 0.5 to 2.0 for the period ratio is negligible. Consequently, the amplification factor ( $a_c$ ) can be calculated by Eq. (3.6) and is shown in Fig. 3-2.

**Structure Yielding Effect.** Limited investigations on the structure yielding effect [9,22] consistently demonstrate a reduction of the dynamic response of an equipment when the supporting structure behaves inelastically during severe earthquakes. The introduction of the response modification coefficient ( $R_s$ ) is attributed to the different degrees of ductility capacities of structures. On the other hand, information on equipment response reduction due to structural yielding is less than that available for the structure itself [17]. It seems reasonable to define the available reduction coefficient ( $R_s$ ) for nonstructural component design as a value ranging from 1.0 to 2.0, which is Eq. (3.7).

### 3.2.2 Experimental Results

Compared with extensive analytical work on the structure-equipment system interaction, small-scale or full-scale experimental evidence seems to be scant [9]. Experimental results reported in [14-16,18] played a role in the development of the proposed procedure in this report.

The experimental model used in [15] was a five-story, one-third scale frame structure with first three periods of 0.308, 0.180, and 0.082 seconds. This model structure was subjected to four typical earthquake input signals based on records of historical California earthquakes, i.e., the El Centro 1940 NS component, the Pacoima Dam 1971 S16E component, the Taft 1950 S69E component, and the Parkfield 1966 N65E component. Each signal was run in real time and time-scaled by a factor of  $\sqrt{3}$ , which corresponds to the geometrical scale of the model. The response of the model to these time-scaled inputs should correspond to that of a full-scale structure to the historical earthquakes. Three oscillators, simple vertical cantilevers, were used in the test to simulate light equipment. Oscillators 1 and 2 were attached to the top floor and oscillator 3 was supported at the second floor of the model structure. Their vibrational periods were respectively taken as 0.308, 0.180, and 0.67 seconds, the first two of which were tuned to the first and second modes of the model structure.

The floor amplification factors ( $a_x$ ) at the top and second floors of the model structure as well as the equipment amplification factors ( $a_e$ ) of the three oscillators are calculated and tabulated in Table 3-4 for both real time and time-scaled signals. As one can see, the top floor amplification factor ( $a_5$ ) varies from a low of 2.7 for both the Pacoima Dam time-scaled and the Parkfield real time signals to a high of 4.8 for the El Centro and Parkfield time-scaled signals. These amplifications have a mean of 3.46 and a coefficient of variation of 0.276, which support the maximum value of 3.75 for  $a_n$  in Eq. (3.4). Furthermore, the values of ratio  $a_2/a_5$  in the last column of Table 3-4 have a mean of 0.639, which roughly agrees with the value 0.56 calculated from Eq. (3.3). The larger statistical value of  $a_2/a_5$  from the experimental results may be due to the straight line assumption used for the first mode shape of the experimental structure in Eq. (3.3) as well as higher-mode contribution which is especially significant to the response at lower floors. It can also be observed that values of the equipment amplification factor ( $a_e$ ) have a mean of 2.996 for oscillator 1 tuned to the structural fundamental mode and a mean of 1.913 for oscillator 2 which is detuned to the fundamental mode but tuned to the second mode of the structure. The larger equipment amplification factor (2.431) for oscillator 3 over oscillator 2 further illustrates the higher-mode involvement in lower floor's response.

In the experiment reported in [18], a three-story, one-quarter scaled frame was used to model the building structure and a cantilevered damper was used to represent the component. The shaking table test results show that the interaction effect between structure and equipment is significant in the tuned cases and a numerical calculation scheme can predict equipment response that agrees well with the experimental results.

The floor response spectrum for a full-scaled equipment converted from the scaled model was calculated numerically for different equipment locations and is shown in Fig. 3-8. Obviously, the floor response spectrum strongly depends on the equipment location in tuned cases, which supports the proposed formula of the design force here.

### 3.2.3 Observations on Past Earthquakes

Many observations on the structural behavior during earthquakes have been conducted in the past two decades. Most of them were made in California during a few major earthquakes such as the San Fernando earthquake on February 9, 1971, the Whittier earthquake on October 1, 1987, and the Loma Prieta earthquake on October 17, 1989. These observation data are used here to perform a statistical analysis on the amplification factor ( $a_n$ ) for different types of buildings. Figure 3-9 presents the amplification factors ( $a_n$ ) for different types of buildings (steel frame, reinforced concrete frame, and R-C shear wall) with various structural periods ( $T_s$ ). It can be seen from this plot that the observed data are quite dispersive. This dispersion mainly results from the fact that the soil layer on which the structure is located and the seismic intensity to which the structure is subjected are not distinguished. Different degrees of structural yielding involved during these earthquakes may further complicate the distribution of the observed data. Nevertheless, the proposed floor amplification factor ( $a_n$ ) in Eq. (3.4) for soil conditions of type IV (solid line in Fig. 3-9) almost envelopes the dispersive observation data.

Figure 3-10 presents the same set of observed amplification factors ( $a_n$ ) as a function of building structural period ( $T_s$ ) relative to the different earthquake events. It can be seen that most observed data are from the more recent earthquakes such as the Loma Prieta earthquake.

Similar statistical analyses for the amplification factor have been conducted elsewhere [10,21] and the trapezoidal acceleration distribution along a building height has also been observed.

### 3.2.4 Related Design Codes

As mentioned in Section 2.2, the earlier NEHRP provisions (1985, 1988) employed an amplification factor ( $a_x$ ) to distinguish different degrees of response magnification when an equipment is installed at different floors of a building. The deletion of this factor in the current provisions only reinforces difficulties in reaching a good understanding of the component seismic coefficient ( $C_e$ ). As more experience data about component behavior

during earthquakes are accumulated, a better understanding of the floor amplification factor ( $a_x$ ) can be achieved.

The Japanese code [11] for nonstructural component design also introduces the floor amplification factor ( $a_x$ ) as expressed in Eq. (3.3) but the amplification factor ( $a_n$ ) at the top of a building structure is bounded by a factor of 10/3 instead of  $1.5 \times 2.5 (= 3.75)$  in this report, which is more justifiable. In addition, the expression for  $a_n$  in the Japanese code is independent of soil conditions.

**TABLE 3-1. Response Modification Coefficients**

Basic Structural System and Seismic Force Resisting System	for Component Design, $R_s$	for Structural Design, $R$
<b>Bearing Wall System</b>		
Light frame walls with shear panels	1.8	6.5
Reinforced concrete shear walls	1.5	4.5
Reinforced masonry shear walls	1.4	3.5
Concentrically braced frames	1.4	4.0
Unreinforced masonry shear walls	1.0	1.25
<b>Building Frame System</b>		
Eccentrically braced frames, moment resisting connections at columns away from link	2.0	8.0
Eccentrically braced frames, non-moment resisting connections at columns away from link	1.9	7.0
Light frame walls with shear panels	1.9	7.0
Concentrically braced frames	1.6	5.0
Reinforced concrete shear walls	1.6	5.5
Reinforced masonry shear walls	1.5	4.5
Unreinforced masonry shear walls	1.0	1.5
<b>Moment Resisting Frame System</b>		
Special moment frames of steel	2.0	8.0
Special moment frames of reinforced concrete	2.0	8.0
Intermediate moment frames of reinforced concrete	1.4	4.0
Ordinary moment frames of steel	1.5	4.5
Ordinary moment frames of reinforced concrete	1.1	2.0
<b>Dual System with a Special Moment Frame Capable of Resisting at Least 25% Prescribed Seismic Forces</b>		
Eccentrically braced frames, moment resisting connections at columns away from link	2.0	8.0
Eccentrically braced frames, non-moment resisting connections at columns away from link	1.9	7.0
Concentrically braced frames	1.7	6.0
Reinforced concrete shear walls	2.0	8.0
Reinforced masonry shear walls	1.8	6.5
Wood sheathed shear panels	2.0	8.0
<b>Dual System with an Intermediate Moment Frame of Reinforced Concrete or an Ordinary Moment Frame of Steel Capable of Resisting at Least 25% of Prescribed Seismic Forces</b>		
Concentrically braced frames	1.6	5.0
Reinforced concrete shear walls	1.7	6.0
Reinforced masonry shear walls	1.6	5.0
Wood sheathed shear panels	1.9	7.0
<b>Inverted Pendulum Structures--Seismic Force Resisting System</b>		
Special moment frames of structural steel	1.2	2.5
Special moment frames of reinforced concrete	1.2	2.5
Ordinary moment frames of structural steel	1.0	1.25

**TABLE 3-2. Mechanical and Electrical Component and System Response Modification Coefficient ( $R_c$ ) and Performance Criteria Factor (P)**

Mechanical and Electrical Component or System	Response Modification Coefficient ( $R_c$ )	Performance Criteria Factor (P) [new(old)]			
		Seismic	Hazard	Exposure	Group
		I	II	III	
Fire protection equipment and systems	1.1	1.2(1.5)	1.2(1.5)	1.2(1.5)	
Emergency or standby electrical systems	1.1	1.2(1.5)	1.2(1.5)	1.2(1.5)	
Elevator drive, suspension system, and control anchorage	1.6	1.0	1.0	1.2(1.5)	
General equipment Boilers, furnaces, incinerators, water heaters, and other equipment using combustible energy sources or high temperature energy sources chimneys, flues, smokestacks, and vents Communication systems Electrical bus ducts, conduit, and cable trays Electrical motor control centers, motor control devices, switchgears, transformers, and unit substations Reciprocating or rotating equipment Tanks, heat exchangers, and pressure vessels Utility and service interfaces	1.1	0.8(0.5)	1.0	1.2(1.5)	
Manufacturing and process machinery	2.7	0.8(0.5)	1.0	1.2(1.5)	
Pipe systems Gas and high hazard piping Fire suppression piping Other pipe systems	1.1 1.1 2.7	1.2(1.5) 1.2(1.5) NR	1.2(1.5) 1.2(1.5) 1.0	1.2(1.5) 1.2(1.5) 1.2(1.5)	
HVAC and service ducts	2.7	NR	1.0	1.2(1.5)	
Electrical panel boards and dimmers	2.7	NR	1.0	1.2(1.5)	
Lighting fixtures	2.7	0.8(0.5)	1.0	1.2(1.5)	
Conveyor systems (nonpersonnel)	2.7	NR	NR	1.2(1.5)	

**TABLE 3-3. Architectural Component Response Modification Coefficient ( $R_c$ ) and Performance Criteria Factor (P)**

Architectural Component	Response Modification Coefficient ( $R_c$ )	Performance Criteria Factor (P) [new(old)]			
		Seismic	Hazard	Exposure	Group
		I	II	III	
Exterior nonbearing walls	2.1	1.2(1.5)	1.2(1.5)	1.2(1.5)	
Interior nonbearing walls					
Stair enclosures	1.5	1.0	1.0	1.2(1.5)	
Elevator shaft enclosures	1.5	0.8(0.5)	0.8(0.5)	1.2(1.5)	
Other vertical shaft enclosures	2.1	1.0	1.0	1.2(1.5)	
Other nonbearing walls	2.1	1.0	1.0	1.2(1.5)	
Cantilever elements					
Parapets, chimneys, or stacks	1.0	1.2(1.5)	1.2(1.5)	1.2(1.5)	
Wall attachments (see Sec. 8.2.3)	1.0	1.2(1.5)	1.2(1.5)	1.2(1.5)	
Veneer connections	1.0	0.8(0.5)	1.0	1.0	
Penthouses	3.0	NR	1.0	1.0	
Structural fireproofing	2.1	0.8(0.5)	1.0	1.2(1.5)	
Ceilings					
Fire-rated membrane	2.1	1.0	1.0	1.2(1.5)	
Nonfire-rated membrane	3.0	0.8(0.5)	1.0	1.0	
Storage racks more than 8 feet in height (content included)	1.5	1.0	1.0	1.2(1.5)	
Access floors (supported equipment included)	1.1	0.8(0.5)	1.0	1.2(1.5)	
Elevator and counterweight guideways and supports	1.6	1.0	1.0	1.2(1.5)	
Appendages					
Roofing units	3.0	NR	1.0	1.0	
Containers and miscellaneous components (free standing)	1.5	NR	1.0	1.0	
Partitions					
Horizontal exits including ceiling	2.1	1.0	1.2(1.5)	1.2(1.5)	
Public corridors	2.1	0.8(0.5)	1.0	1.2(1.5)	
Private corridors	3.0	NR	0.8(0.5)	1.2(1.5)	
Full height area separation partitions	2.1	1.0	1.0	1.2(1.5)	
Full height other partitions	3.0	0.8(0.5)	0.8(0.5)	1.2(1.5)	
Partial height partitions	3.0	NR	0.8(0.5)	1.0	



**TABLE 3-4. Floor and Equipment Amplification Factors of a Test Structure**

signal	input	$a_5$ (5th fl)	$a_2$ (2nd fl)	$a_c$ (osc. 1)	$a_c$ (osc. 2)	$a_c$ (osc. 3)	$a_2/a_5$
real time	El Centro	3.890	1.940	2.815	2.030	2.362	0.4986
	Taft	3.454	1.923	5.385	1.643	1.090	0.5567
	Pacoima	3.549	2.126	2.449	2.998	2.547	0.5990
	Parkfield	2.685	1.750	4.215	1.466	3.306	0.6519
time-scaled	El Centro	4.737	2.267	1.626	1.247	0.952	0.4785
	Taft	1.855	1.879	3.687	2.984	4.036	1.0129
	Pacoima	2.706	1.820	1.558	1.503	2.446	0.6728
	Parkfield	4.776	3.058	2.235	1.430	2.709	0.6403
mean		3.460	2.095	2.996	1.913	2.431	0.639
coefficient of variation		0.276	0.189	0.418	0.344	0.396	0.244

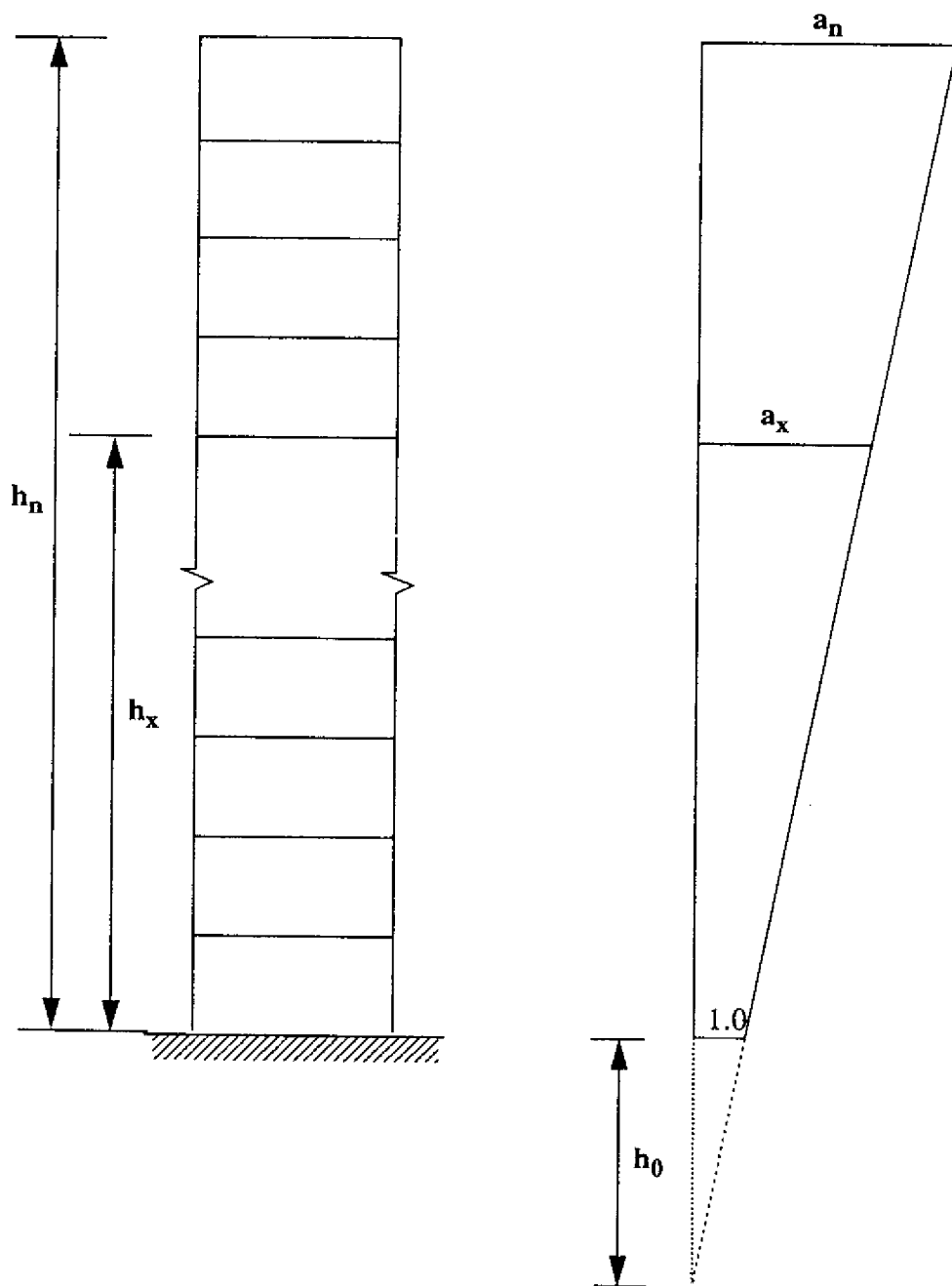


**Fig. 3-1 Building Structure and Floor Amplification Factor**

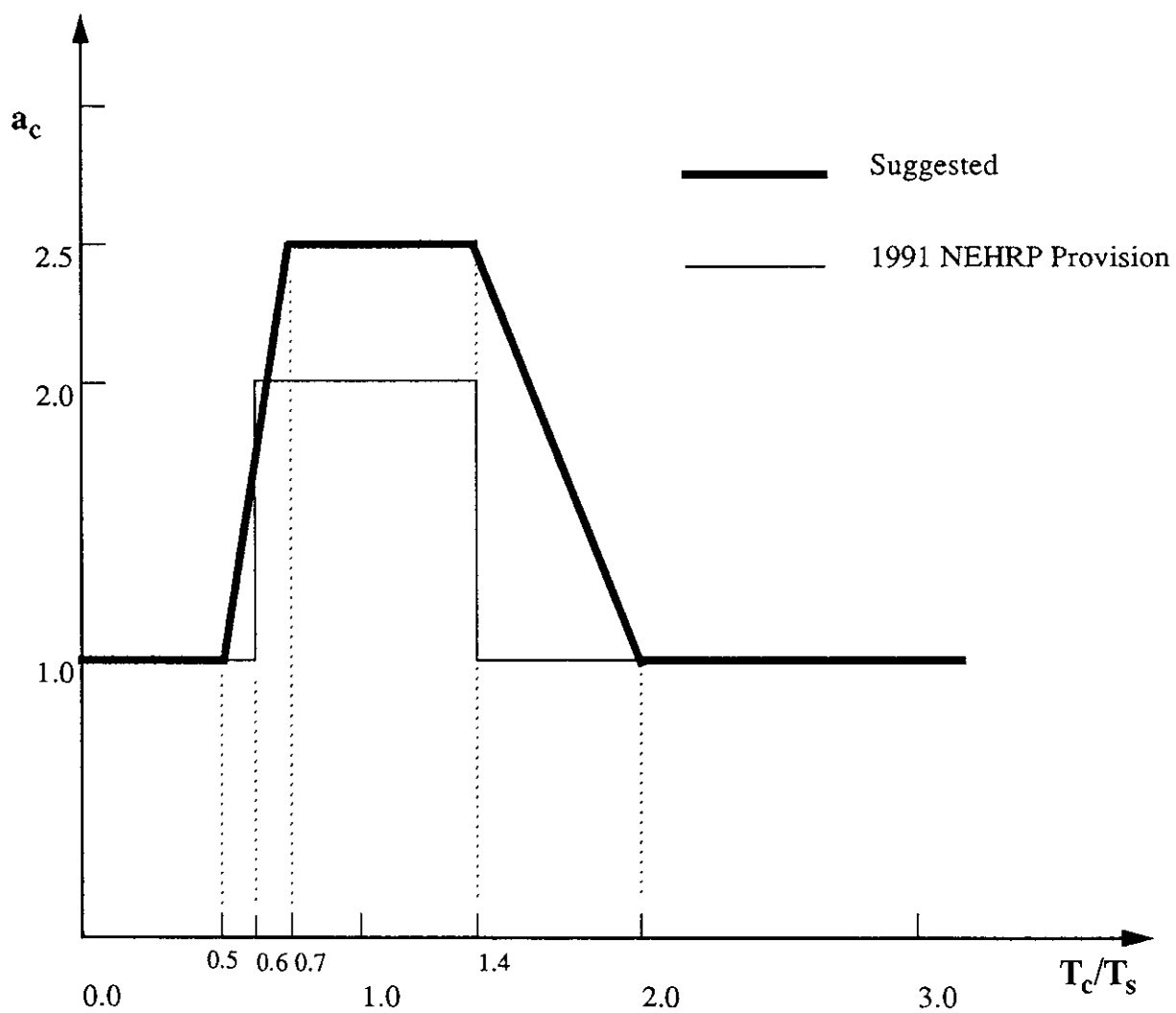


**Fig. 3-2 Equipment Amplification Factor**

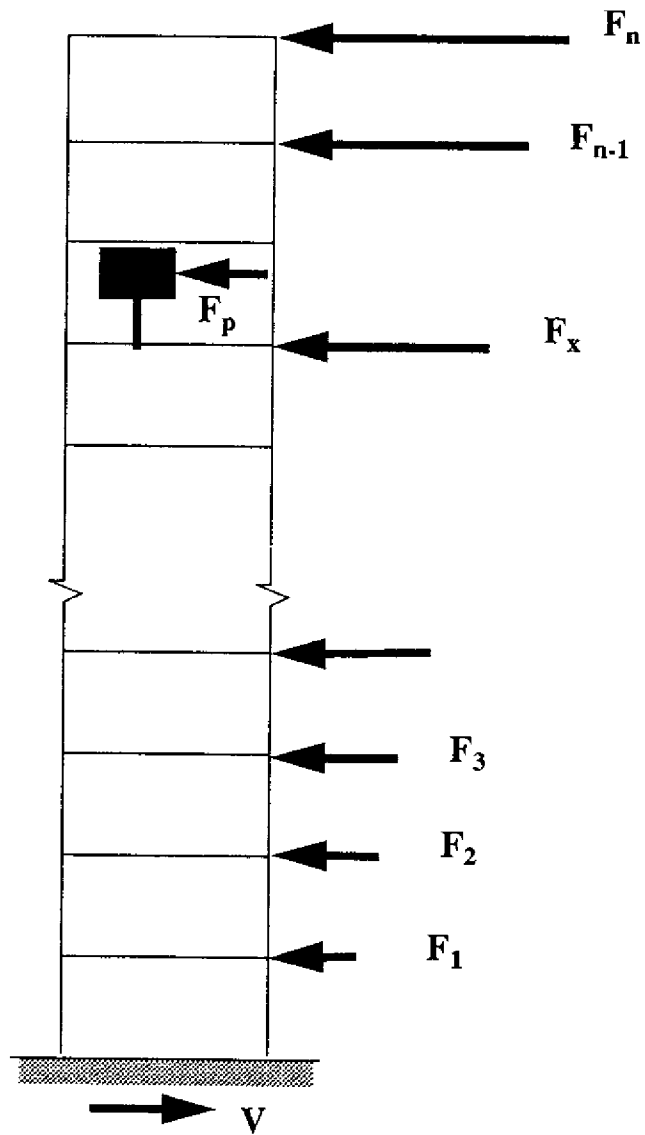


**Fig. 3-3 Force Balance Between Structure and Component**

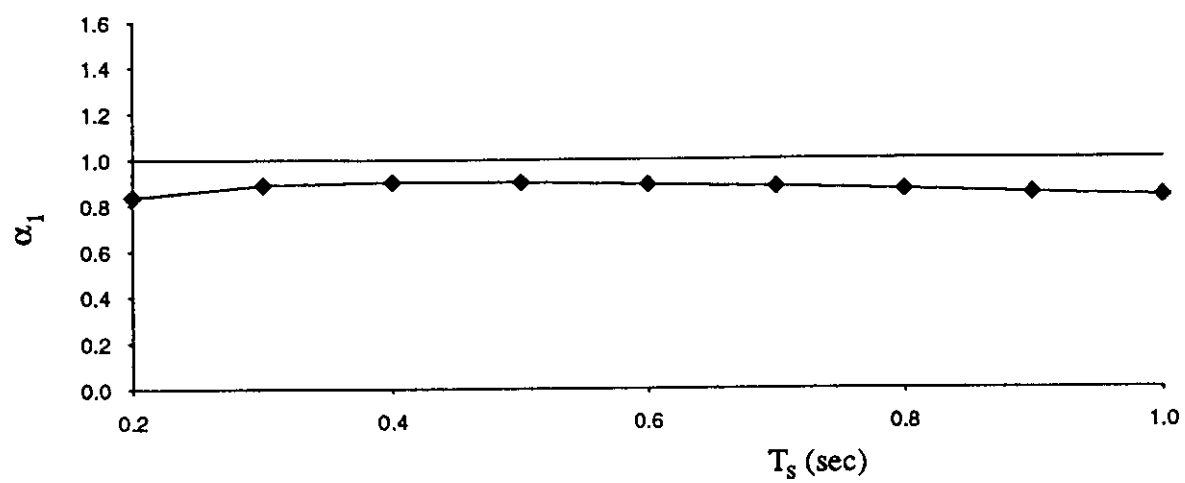


Fig. 3-4 Coefficient  $\alpha_1$

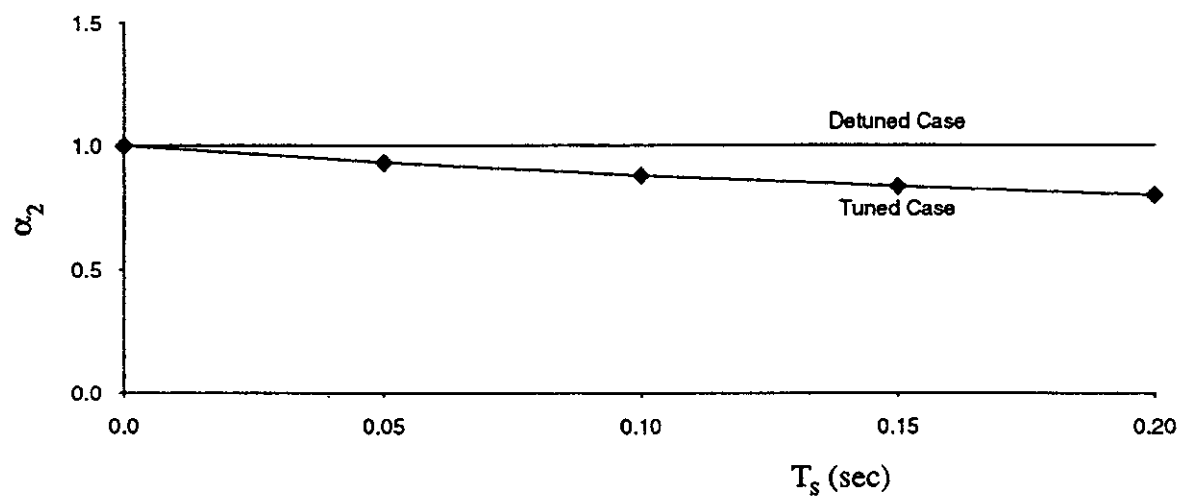


Fig. 3-5 Coefficient  $\alpha_2$

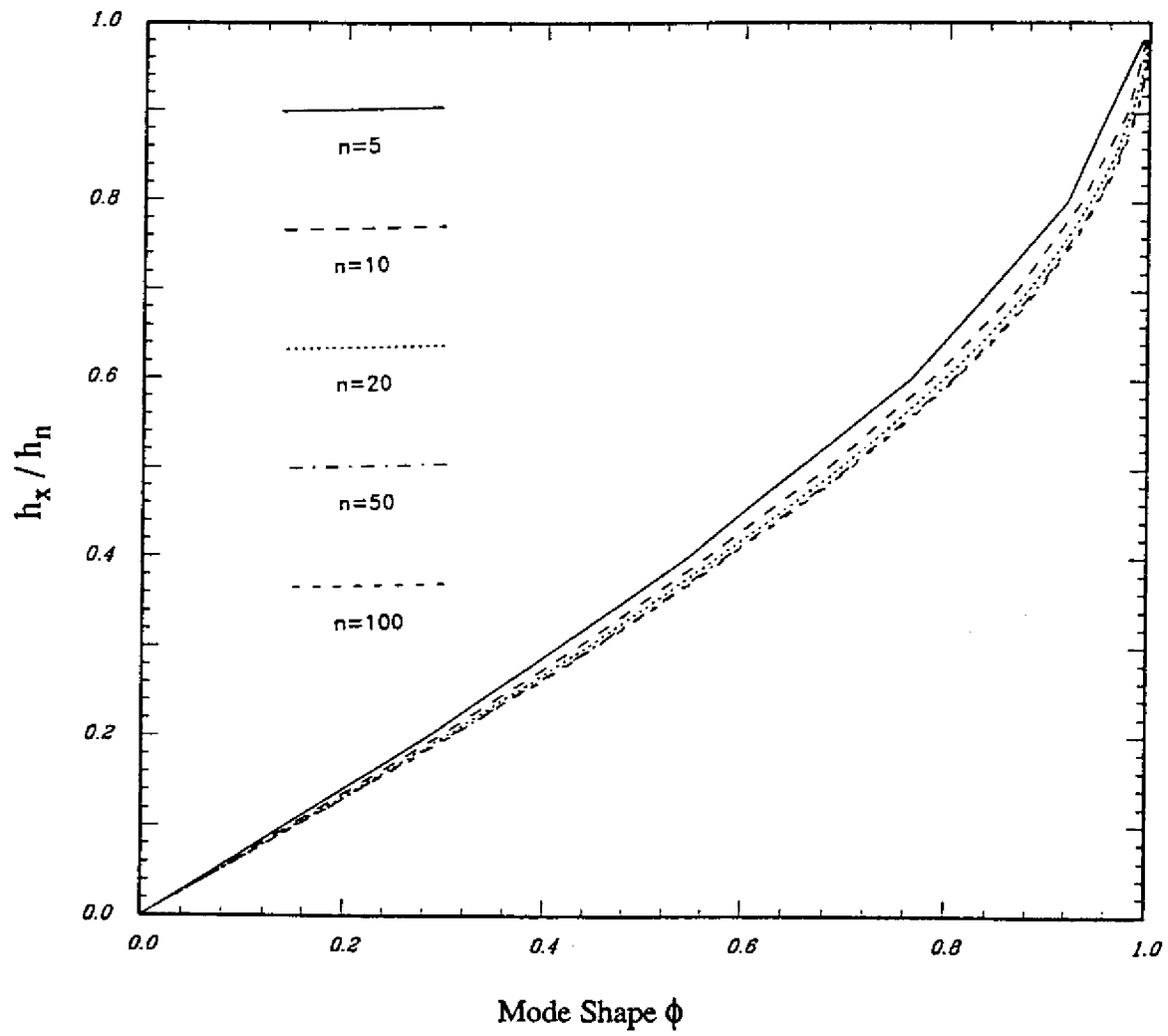


Fig. 3-6 First Mode Shape of a Uniform Moment-Resisting Frame Structure

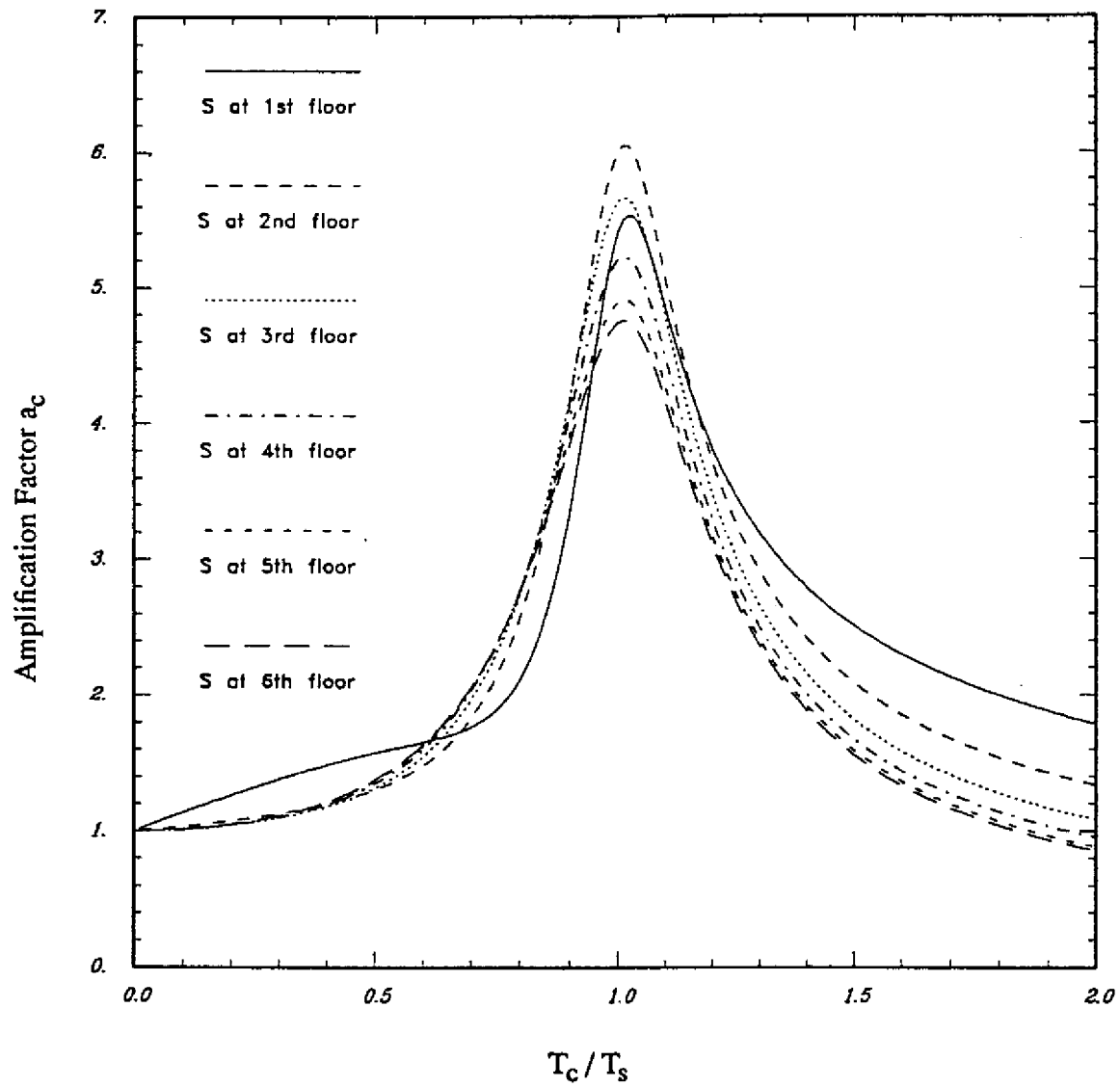


Fig. 3-7 Equipment Amplification Factor of a Six-Story Building:  
5% Damping Ratios for Equipment and Building Structure

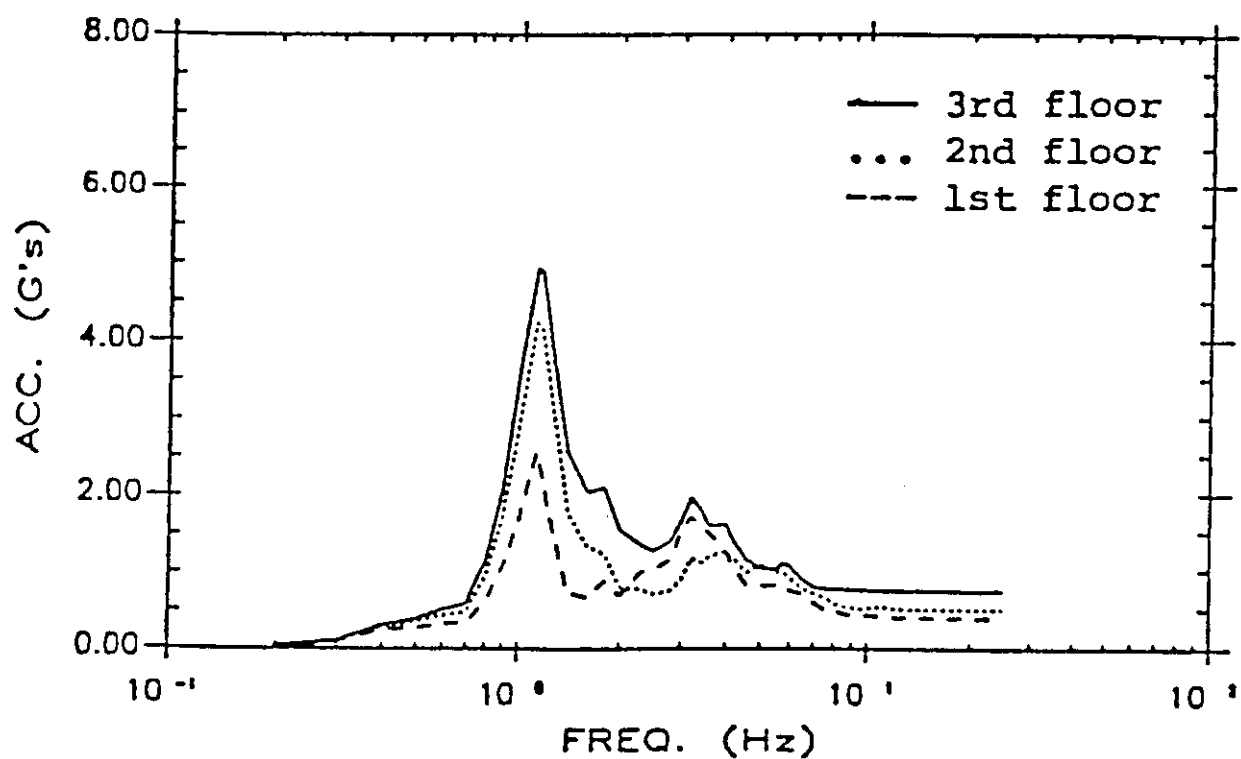


Fig. 3-8 Floor Response Spectrum for Secondary System Attached to Full-Scale Frame Under El-Centro 1940 Earthquake:  
Location Effect (Taken from [18])



Base to Roof Acceleration Amplification Factor--Observation from California Earthquakes

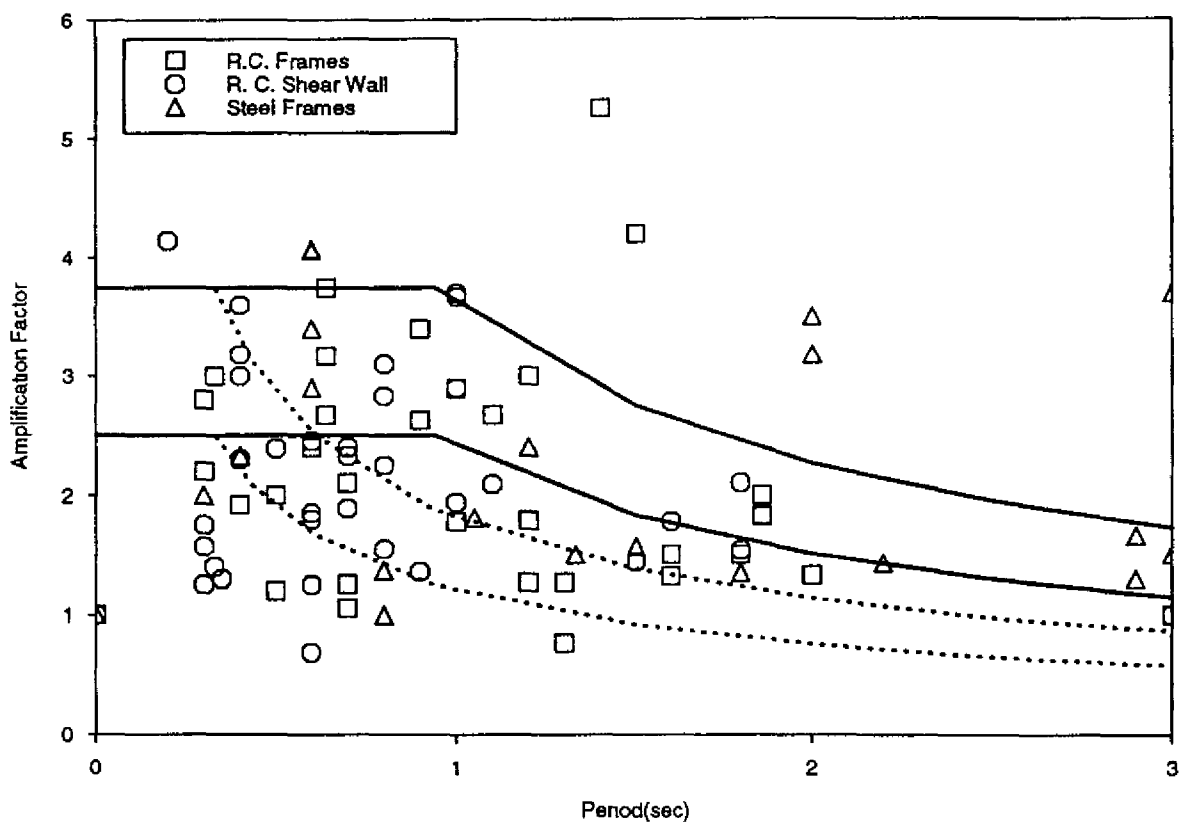


Fig. 3-9 Observation Data (Different Structures)

Base to Roof Acceleration Amplification Factor--Observation from California Earthquakes

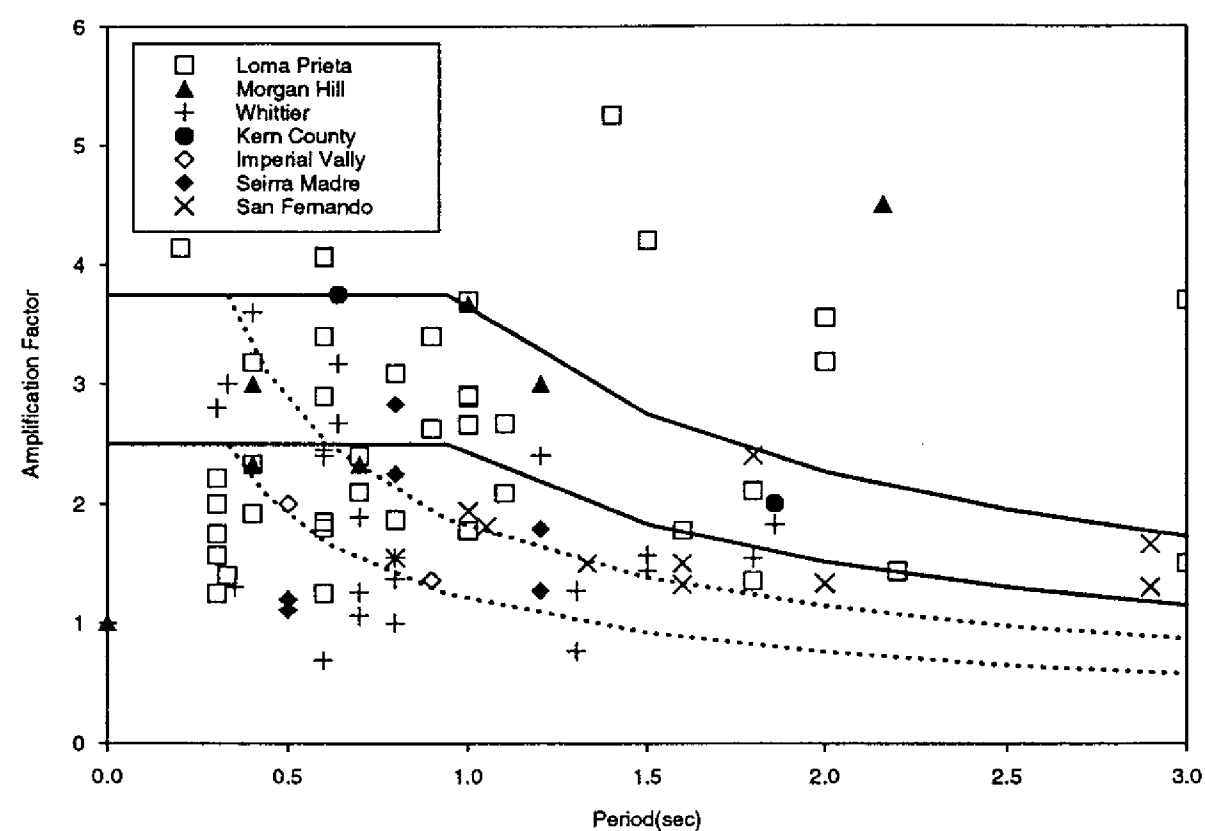


Fig. 3-10 Observation Data (Different Earthquakes)